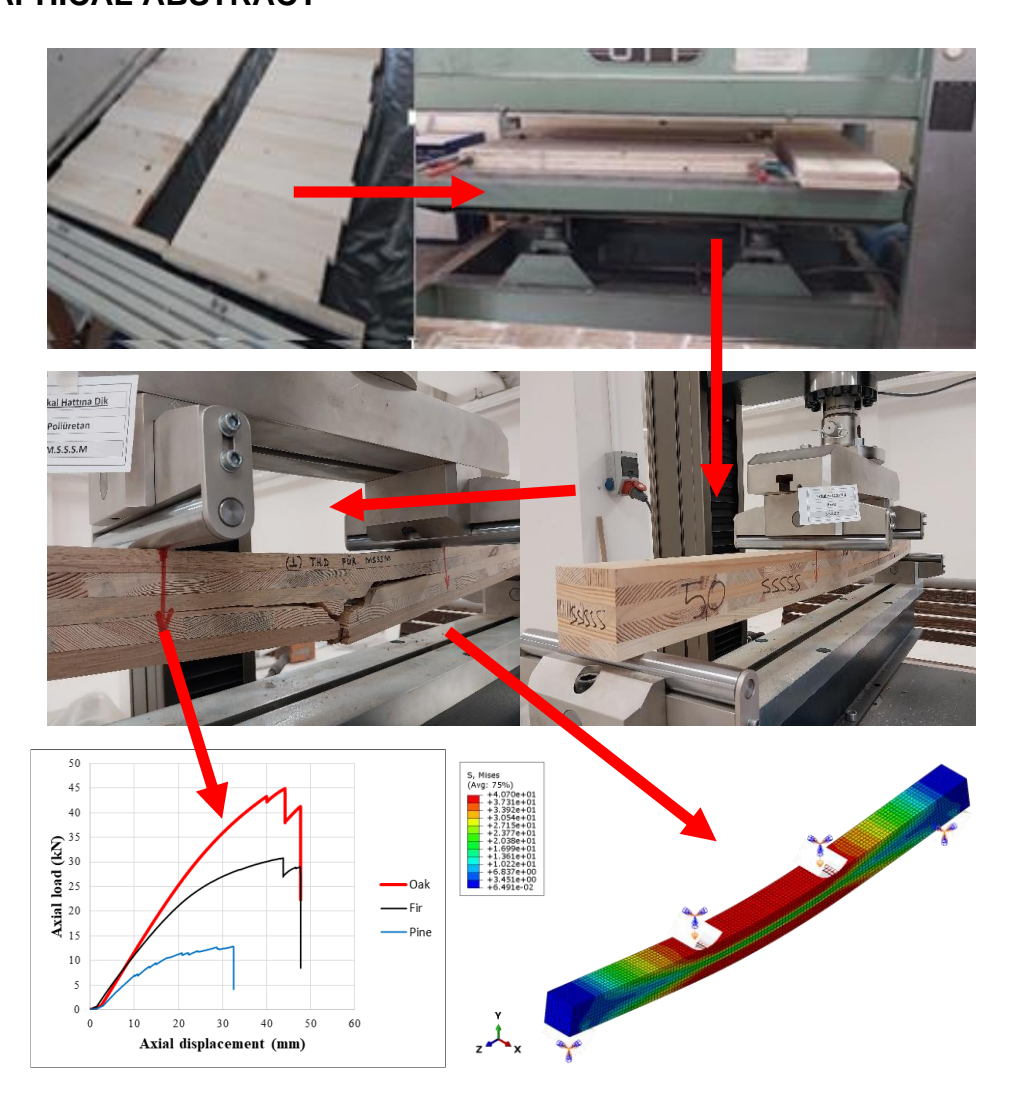
# **Experimental and Numerical Investigations of Glued Cross-Laminated Timber Beams Produced with Different Wood Species and Glues**

Ramazan Bülbül,<sup>a</sup> Hakan Keskin,<sup>a</sup> Musa Kaya,<sup>a</sup> Ömer Mercimek,<sup>b,\*</sup> Abdullah Türer,<sup>c</sup> İrfan Kocaman,<sup>d</sup> Minel Ahu Kara Alaşalvar,<sup>e</sup> and Yağmur Kopraman <sup>a</sup>

DOI: 10.15376/biores.20.2.4720-4745

## **GRAPHICAL ABSTRACT**



<sup>\*</sup> Corresponding author: omercimek@ankara.edu.tr

# Experimental and Numerical Investigations of Glued Cross-Laminated Timber Beams Produced with Different Wood Species and Glues

Ramazan Bülbül,<sup>a</sup> Hakan Keskin,<sup>a</sup> Musa Kaya,<sup>a</sup> Ömer Mercimek,<sup>b,\*</sup> Abdullah Türer,<sup>c</sup> İrfan Kocaman,<sup>d</sup> Minel Ahu Kara Alaşalvar,<sup>e</sup> and Yağmur Kopraman <sup>a</sup>

Five-layer cross-laminated timber (CLT) beams made from 17-mm thick lumber pieces were produced using wood from Scots pine (Pinus sylvestris L.), Uludağ fir (Abies bornmüelleriana Mattf.), and oak (Quercus petraea L.). The outer layers consisted of Scots pine and oak, while the intermediate layers included Scots pine and fir wood. During the layer formation phase in the side-by-side joining press and in the CLT beam formation phase with layers stacked at 90°, polyvinyl acetate (PVAc) and polyurethane (PUR) adhesives were used. After conditioning the CLT beams at 20 °C and 65% relative humidity, their dry density values and results from a four-point bending test perpendicular to the adhesive line, including max load, displacement at max load, stiffness, max displacement, and energy dissipation capacity, were evaluated and compared with those obtained using ABAQUS finite element software. The results revealed that timber species, adhesive type, and perforation significantly influenced the mechanical behavior of CLT beams, with oakbased specimens generally outperforming fir and pine in load-bearing capacity. The findings contribute valuable insights into the optimization of CLT beam design for structural applications.

DOI: 10.15376/biores.20.2.4720-4745

Keywords: Cross laminated timber beam; 4-Point bending; Pine; Oak; Fir; Adhesive; Species

Contact information: a: Department of Civil Engineering, Gazi University, Ankara, Türkiye; b: Department of Civil Engineering, Ankara University, Ankara, Türkiye; c: Department of Civil Engineering, Ankara Yıldırım Beyazıt University, Ankara, Türkiye; d: Department of Civil Engineering, Erzurum Technical University, Erzurum, Türkiye; e: Department of Architecture, Harran University, Şanlıurfa, Türkiye; \*Corresponding author: omercimek@ankara.edu.tr

#### INTRODUCTION

Wood as a material has been widely used in structural applications and furniture manufacturing since the beginning of humanity because of its aesthetic appearance, naturalness, mechanical resistance adequacy, and ease of processing for construction and craftsmanship. The increasing use of timber materials in parallel with the world population has led to the rapid consumption of existing forests on Earth. Therefore, to ensure the sustainability of the world's forest resources in the supply-demand interaction, efforts to develop engineered timber-based products have gained momentum with the impact of technological advancements.

Engineered timber products, such as cross-laminated timber (CLT), are important for high-rise buildings due to their carbon storage capacity (Perez *et al.* 2005), fire resistance, superior properties against wind and seismic effects, and competitive cost performances (Abed *et al.* 2022). Common engineered timber-based products used in

structural applications include plywood (PW), oriented strand board (OSB), cross-laminated timber beams (CLT), and glued laminated timber (Glulam) (Milner 2009; Mercimek *et al.* 2024). Timber is also used as formwork and supporting beams for reinforced concrete structures. Although studies on timber formwork beams (Dönmez *et al.* 2022; Türer *et al.* 2024)) are limited, they are significant structural elements in terms of load-bearing capacity.

Cross-laminated timber beams are an industrial product related to traditional sawing technologies from Scandinavia and Europe. Modern CLT beams were developed in the mid-1990s through collaboration between industry and academia in Austria as an alternative to concrete and steel materials and as wall beams to resist horizontal loads based on rigidity and stability in multi-story timber structures (Brandner *et al.* 2016; Waugh Thistleton Architects 2018; Ceylan 2021).

The CLT producers in Europe and Canada typically use spruce, pine, and fir wood, while Douglas-fir, spruce, and larch are common in the United States, and pine is widely used in Australia and New Zealand. Additionally, the availability of different timber species to meet the growing demand in the timber construction sector in these regions is being explored (Gavric 2013; He *et al.* 2018). A study conducted in Italy also used regional chestnut and poplar trees in the production of non-load-bearing CLT beams (Callegari *et al.* 2010).

The CLT beams are engineered timber beams obtained by stacking timber layers with their grain directions perpendicular to each other using certain adhesives, ranging from a minimum of 3 layers to up to 7 layers (Yesügey *et al.* 2014; He *et al.* 2018). CLT is used in various structural applications, including walls, floors, and roofs in high-rise buildings. It is also used in interior decoration for walls, stairs, furniture, and other decorative elements. CLT can be used for making beams, columns, and other structural elements.

Advantages of using CLT include its high strength and rigidity, despite being lighter than steel, making it a lighter and more sustainable building material. It is resistant to fire, insects, and decay while maintaining the natural beauty of timber. The disadvantages of CLT include higher costs compared to traditional building materials. The investment costs for a CLT production facility exceed those for other construction systems, and CLT processing differs from traditional timber, requiring integrated production processes and facility setup.

In determining the dimensional limits of CLT beams, factors such as the distance of the production line, methods of transporting finished products to the construction site, and physical conditions at the site are crucial. Although CLT beams vary among manufacturers, their widths typically range from 0.6 m to 2.95 m, with a maximum of up to 4 m, and lengths can reach up to 24 m with length joints. Thicknesses range from 5 cm to 50.8 cm, depending on design and structural system requirements (Crespell and Gagnon 2010; FPInnovations 2011; ANSI/APA PRG 320 2018).

In the production of timber-based structural products, adhesives that provide the connection between layers and significantly affect mechanical strength are typically formaldehyde-based; these include urea, melamine, resorcinol, or phenol resins. For manufacturing CLT beams, phenol-resorcinol formaldehyde (PRF), polyurethane (PUR), and melamine-urea formaldehyde (MUF) adhesives are commonly used. However, today, the use of polyurethane (PUR) adhesives that are free from solvents and formaldehyde is becoming more prevalent (BS EN 301 2006; Lehmann 2013).

During the production of CLT, low-density and high-resistance materials are targeted by using timber materials of different densities for the outer and intermediate layers. Therefore, the density factor is quite important. CLT, which can be used as wall and flooring elements in wooden structures, has been produced using Scots pine, fir, and oak timbers. Perforation applications at 10% and 20% were applied to the middle layers of CLT, and five-layer experimental specimens were prepared.

In this study, some physical and mechanical properties of five-layer crosslaminated timber beams and adhesives produced using different wood types (oak, Scots pine, and fir) were considered. The values of maximum load, displacement at maximum load, stiffness, maximum displacement, and energy dissipation capacity obtained from a four-point bending test perpendicular to the adhesive line were numerically tested and compared using ABAQUS finite element software. Experimental studies were also conducted parallel to the adhesive line, and comparisons were made with the values obtained in the perpendicular direction. This study offers several innovative contributions to the design and analysis of CLT beams. Investigations into the effects of density variations on mechanical performance are made possible using layered combinations of Scots pine, fir, and oak. The use of 10% and 20% core-layer perforations provides a novel way to improve energy dissipation. Current information on environmentally friendly bonding techniques can be obtained by directly comparing PVAc and formaldehyde-free PUR adhesives under the same circumstances. Furthermore, the predictive understanding of CLT behavior is strengthened by combining experimental results with numerical modeling based on ABAQUS.

#### **EXPERIMENTAL**

## **Test Specimens and Materials**

In this study, five-layer CLT beams were produced using wood from oak (Quercus L.), fir (Abies sp. L.), and Scots pine (Pinus sylvestris). The kiln-dried and planed boards of wood used in this study were obtained from a nearby commercial wood supplier in Türkiye. Before processing, all wood was conditioned to achieve a moisture content of about 12% that was appropriate for structural uses. To ensure that the boards were free of defects such as knots, cracks, decay, insect damage, and reaction wood, they were carefully chosen and prepared to meet first-grade quality standards. The mechanical performance of the final CLT beams was guaranteed to be consistent and dependable thanks to this sourcing technique. Scots pine is a slender-trunked, sharp-topped tree with thin branches or a robust, smooth-trunked evergreen tree. It is predominantly found in the inner regions of Northern Anatolia and extends into Central Anatolia. Depending on the ecological conditions of its wide range, it can grow between 20 to 50 m tall. Its wood provides a smooth and glossy surface suitable for various uses. It absorbs paint, varnish, and glue easily, and it holds nails well. Due to these properties, Scots pine is used in construction materials, furniture, and carving, including doors, windows, ceilings, and floor coverings. Physical and mechanical properties of Scots pine are given in Table 1. The mechanical and physical properties of Scots pine, oak, and fir presented in Tables 1 through 4 were compiled from previous studies and standard (Ross 2010; Sonderegger et al. 2015; Mercimek et al. 2024).

		1	,
Remarks	Symbol	Value	Unit
Donaite	ρk	490	kg/m³
Density	ho12	520	kg/m³
	$oldsymbol{eta}_{ ext{r}}$	4.0	%
Contraction Coefficient	$oldsymbol{eta}_{t}$	7.7	%
	$oldsymbol{eta}_{ee}$	12.1	%
	E <sub>1,mean</sub>	11700	MPa
Elastic Modulus	E <sub>2,mean</sub>	886	MPa
	E <sub>3,mean</sub>	554	MPa
	G <sub>1,mean</sub>	731.25	MPa
Shear Modulus	G <sub>2,mean</sub>	725	MPa
	G <sub>3,mean</sub>	79	MPa
	<i>V</i> 1	0.37	
Poisson's Ratio	<i>V</i> 2	0.42	
	<i>V</i> 3	0.47	
Bending Strength	$f_{m,k}$	98	MPa
Tension strength	<i>f</i> t,0,k	102	MPa
Compression strength	fook	54	MPa

**Table 1.** Mechanical Properties of Pine (*Pinus sylvestris*)

Fir produces a long, smooth, and robust trunk with a pointed top and has a taproot system. Uludağ fir (*Abies bornmüelleriana* Mattf.) is the fir species in Türkiye with the widest geographic variation among native fir species. Fir is used as a construction material in furniture, beaming, moldings, and veneer production, as well as in making boxes, crates, barrels, toys, and other items. Physical and mechanical properties of fir wood are given in Table 2.

Table 2	. Mechanical	Properties of	f Fir (Abies	bornmüelleriana Mattf.)
I UNIC E	. IVICOHAHIOAI	1 100011100		DOLLING ACTION AT IN A TRIATER.

Remarks	Symbol	Value	Unit
Donoity	<b>/</b> 0k	400	kg/m³
Density	ho12	500	kg/m³
	$oldsymbol{eta}_{ m r}$	3-5	%
Contraction Coefficient	$oldsymbol{eta}_{t}$	6-8	%
	$oldsymbol{eta}_{ee}$	8-12	%
	E <sub>1,mean</sub>	12532	MPa
Elastic Modulus	E <sub>2,mean</sub>	1211	MPa
	E <sub>3,mean</sub>	705	MPa
	G <sub>1,mean</sub>	802	MPa
Shear Modulus	$G_{2,mean}$	851	MPa
	G <sub>3,mean</sub>	85	MPa
	<i>V</i> 1	0.37	
Poisson's Ratio	<i>V</i> 2	0.42	
	<i>V</i> 3	0.47	
Bending Strength	f <sub>m,k</sub>	80-90	MPa
Tension Strength	<i>f</i> t,0,k	90-102	MPa
Compression Strength	<i>f</i> <sub>c,0,k</sub>	45-54	MPa

Oak is found throughout Türkiye, with variations depending on the species. Most oaks are trees, while some are tall shrubs, shedding leaves in winter or remaining evergreen. Oak wood is used in solid and veneered furniture, carving, joinery, and plywood production. It also has a wide range of applications in agricultural tools, flooring,

scaffolding, ceilings, and floor coverings. Physical and mechanical properties of oak wood are provided in Table 3.

Symbol Value Unit Remarks Density 0.69 g/cm<sup>3</sup> **P**12 0.65 g/cm<sup>3</sup>  $\rho_0$ **Contraction Coefficient** 4.0 %  $\beta_r$ %  $\beta_t$ 7.7 12.1 %  $\beta_{V}$ N/mm<sup>2</sup> Elastic Modulus 13 500  $\sigma_{E}$ N/mm<sup>2</sup> Compression Strength  $\sigma_{\rm C}$ 61 Bending Strength  $\sigma_{\mathsf{B}}$ 88 N/mm<sup>2</sup> Dynamic Bending Resistance N/mm<sup>2</sup> 6  $\sigma_{ extsf{DB}}$ Tension Strength 90 N/mm<sup>2</sup>  $\sigma_{\text{c}}$ **Brinell Hardness** N/mm<sup>2</sup> 0// 66 N/mm<sup>2</sup> 9⊤ 34

**Table 3.** Mechanical Properties of Oak (Quercus petraea)

In the production of CLT beams, adhesives used include APEL brand polyurethane (PUR) and polyvinyl acetate (PVAc) adhesives. Polyurethane (PUR) adhesive is a honeycolored, single-component, solvent-free wood adhesive with very high temperature and water resistance. Its applications include door and window bonding, wood laminates, and wood-based material bonding, as well as exterior connections, and bonding of ceramic, concrete, and rigid foam materials. Polyvinyl acetate adhesive is a single-component, solvent-free adhesive preferred for assembly work, known for its ease of application, quick setting, non-odor, and non-flammability, and does not wear out cutting tools during processing. However, PVAc has limited mechanical resistance and tends to soften as temperatures increase, failing to perform its bonding function effectively above 70 °C. Plastic adhesives, which have high resistance to mold and bacteria, are generally used in wood bonding processes and are available for furniture assembly and veneer bonding.

 Table 4. Some Properties of the Materials Used in the Production of CLT Beams

No	Materials	Dimensions (mm)	Density	Humidity
1	Fir	22 × 100 × 1450	0.44	11.3%
2	Oak	22 × 100 × 1450	0.75	12.4%
3	Pine	22 × 100 × 1450	0.59	11.8%
4	PUR	100-130 g/m <sup>2</sup>	1.10	-
5	PVAc	110-120 a/m²	1.08	-

Some properties of the materials used in the formation of five-layer CLT beams are provided in Table 4. Detailed information on the names and characteristics of the test specimens is given in Table 5. Specimen names are given using the initials of the timber type used from outside to inside. The timber species in the outer layer are the same. For example, PFFFP represents a specimen with outer layers of Pine (P) and inner layers of Fir (F); OPPPO represents a specimen with outer layers of Oak (O) and inner layers of Pine (P). The control specimens were prepared from solid wood boards without any adhesive bonding. Each control specimen consisted of a monolithic solid wood element, rather than an assembly of individual 17-mm-thick layers. The total thickness of the control specimens was designed to match exactly the overall thickness of the corresponding CLT specimens, including the cumulative thickness contributed by the glue lines. Specifically, the control

specimens were manufactured as solid members with the same nominal dimensions (length, width, and thickness) as the CLT specimens to ensure fair comparison of their mechanical performance.

Load Direction | Glue Type | Outer Timber Specimen # Name Inner Timber Fir-C 1 2 Oak-C Control solid wood 3 Pine-C 4 **OPPPO** Oak Pine PPPPP 5 Pine Pine **PUR** 6 OFFFO Oak Fir Perpendicular 7 PFFFP Pine Fir to the glue OPPPO-2 8 Oak Pine line PPPPP-2 Pine 9 Pine **PVAc** 10 OFFFO-2 Oak Fir 11 PFFFP-2 Pine Fir OPPPO Pine 12 Oak PPPPP 13 Pine Pine PUR OFFFO 14 Oak Fir 15 **PFFFP** Parallel to the Pine Fir 16 OPPPO-2 glue line Oak Pine PPPPP-2 17 Pine Pine **PVAc** OFFFO-2 18 Oak Fir

**Table 5.** Properties of Test Specimens

#### **Production of Cross Laminated Timber Beams**

PFFFP-2

19

The solid pieces used to form the CLT beams were cut to rough dimensions of 22 mm  $\times$  100 mm  $\times$  1450 mm and then trimmed and cleaned to a final size of 17 mm  $\times$  85 mm  $\times$  1350 mm. The trimmed solid wood pieces were conditioned in a climate chamber at 20 °C and 65% relative humidity until they reached a constant weight. Depending on the type of adhesive used, 100 to 130 g of PVAc and PUR adhesives per square meter were applied to the edges of the conditioned solid pieces. The beams were then assembled by gluing side-by-side using the press machine shown in Fig. 1a, resulting in the layer stacks of CLT beams.

Pine

Fir

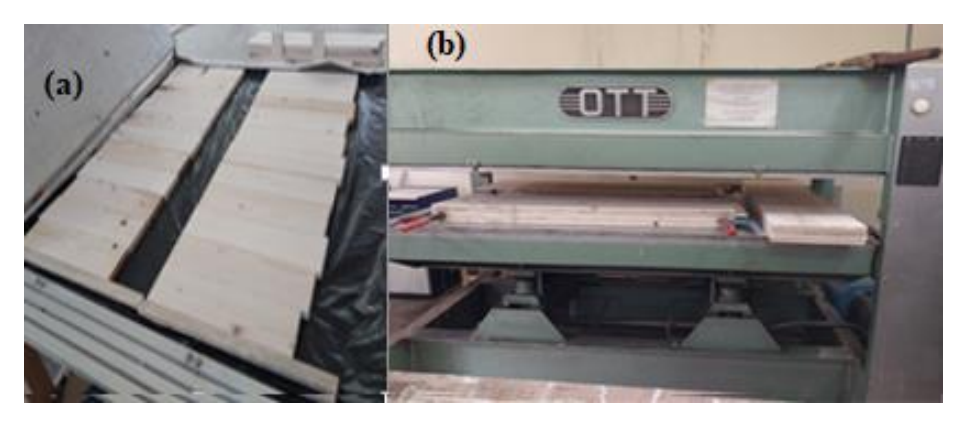


**Fig. 1.** (a) Side-by-side splicing of cross-laminated timber layers, (b) Side-by-side squeezing of cross-laminated timber with a hydraulic press machine

For the CLT beams, the adhesive was applied to one surface of the outer layer boards and to both surfaces of the inner layer boards at the amounts specified in Table 4. The beams were then pressed with a pressure of 8 kg/cm<sup>2</sup> for 12 h using the hydraulic press machine shown in Fig. 1b, resulting in the final CLT beams.

## **Test Setup and Instrumentations**

In the experimental study, an electromechanical loading system with a capacity of 300 kN was used to conduct four-point bending tests as shown in Fig. 2. The four-point configuration enables a clearer assessment of the beam's true bending strength without the influence of localized loading. Thus, the selected method offers more representative and reliable results for structural applications. The test system used is a computer-connected mechanism that allows for load and displacement-controlled tests, as well as tests at a constant loading rate. During the experimental study, a load was applied to the test specimens using a 300 kN capacity electromechanical system. The loading rate was kept constant at 10 mm/min for all specimens. The loading was continued until a failure occurred in the wooden beam test specimens. During the tests, the load and mid-point displacement values were recorded, and the tests were conducted by monitoring the load-midpoint displacement graph.

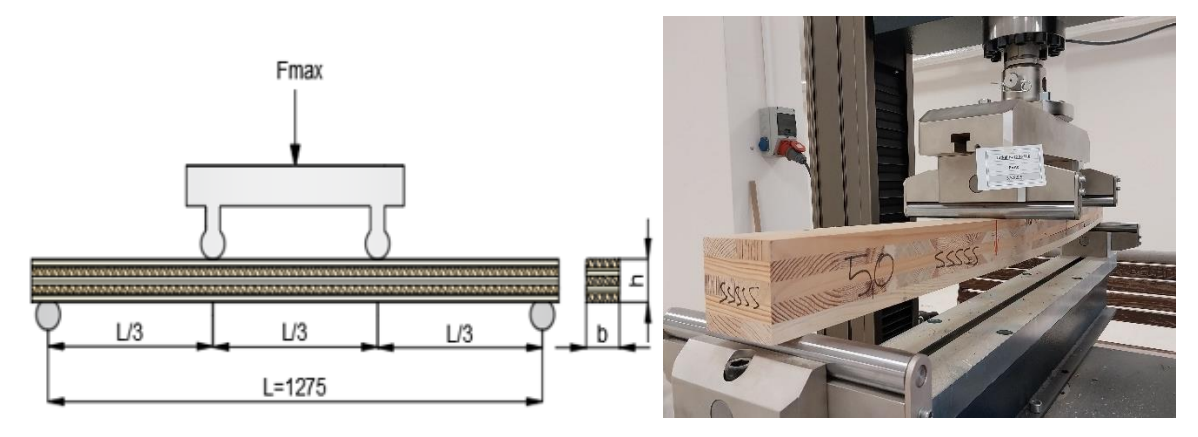


Fig. 2. Four-point bending test setup

#### RESULTS AND DISCUSSION

The results of mechanical performance tests on five-layer cross-laminated timber (CLT) beams made with different mixes of oak, Scots pine, and fir wood are shown in this section. Two distinct adhesives, polyvinyl acetate (PVAc) and polyurethane (PUR), were used to bond the specimens, and their structural behavior was evaluated by subjecting them to four-point bending. The impact of perforation applied to intermediate layers was investigated as a third variable, in addition to the type of adhesive and the species of timber. Based on their importance in maximizing strength, stiffness, and energy dissipation in engineered timber systems, these design parameters were chosen. To compare mechanical behavior in various loading orientations, a set of eight specimens was assessed parallel to the adhesive line, while a total of eleven specimen configurations were tested perpendicular to the adhesive line. The results of the tests were examined in terms of stiffness, maximum

displacement, energy dissipation capacity, displacement at peak load, and maximum load-bearing capacity. A comparative analysis of these findings and an interpretation of the structural implications of each design parameter are given in the ensuing subsections.

Experimental photographs showing the failure modes of specimens with PUR adhesive are given in Fig. 3. Failure modes of specimens with PVAc Adhesive are given in Fig. 4.



**OPPPO Specimen** 

**PPPP Specimen** 



**OFFFO Specimen** 



**PFFFP Specimen** 

Fig. 3. Failure modes of specimens with PUR adhesive

In this study, the mechanical performances of different timber species and adhesive types were evaluated, with a focus on maximum load, displacement at maximum load, stiffness, maximum displacement, and energy dissipation capacity. The experimental specimens were categorized into two primary groups based on the adhesive type: PUR and PVAc, with further differentiation based on the timber species.

## **Comparison of Timber Species Without Adhesive (Solid Wood)**

Among the control specimens that did not use any adhesive, significant variations in mechanical properties were observed. The "Oak-C" specimen exhibited the highest maximum load (45.0 kN) and stiffness (1.02 kN/mm), outperforming both the "Fir-C" and "Pine-C" specimens. Specifically, "Oak-C" had a maximum load that was approximately

46% higher than "Fir-C" (30.8 kN) and 250% higher than "Pine-C" (12.9 kN). This suggests that the oak timber has a substantially higher load-bearing capacity compared to Fir and Pine, making it a more suitable material for applications requiring high strength.



OPPPO Specimen

**PPPPP Specimen** 





**OFFFO Specimen** 

**PFFFP Specimen** 

Fig. 4. Failure modes of specimens with PVAc adhesive

## **Comparison of Adhesives**

When comparing the specimens with PUR adhesive, notable differences in performance were also evident. The "PPPP" specimen, which had pine layers throughout, achieved a maximum load of 16.0 kN, which was 3% higher than the "PFFP" specimen (15.9 kN), but significantly lower than the control "Oak-C" specimen. However, the introduction of perforation in specimens such as "OFFFO" led to substantial reductions in performance. For instance, the "OFFFO" specimen displayed a maximum load of only 8.95 kN, which is 44% lower than what was observed in the non-perforated "OPPPO" specimen (16.5 kN). Additionally, the energy dissipation capacity of "OFFFO" (179 kN/mm) was significantly lower compared to the "OPPPO" specimen (293 kN/mm), indicating that perforation negatively affects the ability of the material to absorb energy under loading.

The ultimate load capacity of the PUR-bonded specimen with fir inner layers (PFFFP) decreased by 0.6% compared to the PUR-bonded specimen with pine inner layers (PPPPP). The displacement at maximum load in the PUR-bonded specimen with fir inner layers (PFFFP) decreased by 19% compared to the PUR-bonded specimen with pine inner layers (PPPPP). The initial stiffness of the PUR-bonded specimen with fir inner layers

(PFFFP) increased by 5% compared to the PUR-bonded specimen with pine inner layers (PPPPP). The maximum displacement observed in the PUR-bonded specimen with fir inner layers (PFFFP) decreased by 6% compared to the PUR-bonded specimen with pine inner layers (PPPPP). The energy dissipation capacity of the PUR-bonded specimen with fir inner layers (PFFFP) decreased by 3% compared to the PUR-bonded specimen with pine inner layers (PPPPP).

The specimens with PVAc adhesive displayed varying degrees of mechanical performance, influenced by both the timber species and the degree of perforation. The "PFFP-2" specimen, with a maximum load of 15.86 kN and a stiffness of 0.83 kN/mm, outperformed the "OFFFO-2" specimen, which had a maximum load of 8.95 kN and a stiffness of 0.61 kN/mm. Interestingly, despite having similar maximum loads, the "OPPPO-2" specimen exhibited a 25% higher stiffness compared to "OFFFO-2," suggesting that the configuration of perforations within the material plays a critical role in determining stiffness. The displacement at maximum load of the PVAc-bonded specimen with fir inner layers (PFFFP-2) increased by 3% compared to the PVAc-bonded specimen with pine inner layers (PPPPP-2). Conversely, the initial stiffness of the PVAc-bonded specimen with pine inner layers (PFFFP-2) decreased by 5% compared to the PVAc-bonded specimen with pine inner layers (PPPPP-2). Similarly, the energy dissipation capacity of the PVAc-bonded specimen with fir inner layers (PFFFP-2) decreased by 3% relative to the PVAc-bonded specimen with pine inner layers (PFFFP-2) decreased by 3% relative to the PVAc-bonded specimen with pine inner layers (PFFPP-2).

## **Ultimate Load Capacity**

The "Oak-C" specimen, which used oak as the outer layer and no adhesive, exhibited the highest ultimate load capacity at 45.0 kN. Compared to the "Fir-C" specimen, this represents a significant increase of 46%. The "OPPPO" beam, with oak as the outer layer and pine as the inner layers, achieved an ultimate load capacity of 16.5 kN when bonded with PUR, which is approximately 28% higher than the "OFFFO" beam that had fir as the outer and inner layers, which recorded an ultimate load of 8.95 kN. For the "PFFFP" beam, the ultimate load was 15.9 kN, showing a 2% increase compared to the "PPPPP-2" beam (16.0 kN) with PVAc adhesive and pine layers.

# **Displacement at Ultimate Load**

The displacement at ultimate load for "Oak-C" was 44.2 mm, only slightly higher than "Fir-C" at 43.7 mm, indicating a 1% difference. The "OPPPO" beam with PUR had a displacement of 26.9 mm, which is 44% greater than the "OFFFO" beam's displacement of 18.36 mm. "PFFFP-2" with PVAc had a displacement of 19.0 mm, a 4% decrease compared to "PPPPP-2" which had a displacement of 18.4 mm.

### **Initial Stiffness**

The "Oak-C" beam had the highest initial stiffness at 1.02 kN/mm, which is 46% higher than the "Fir-C" beam at 0.70 kN/mm. The "OPPPO" beam with PUR adhesive had an initial stiffness of 0.61 kN/mm, which was 19% lower than the "OFFFO" beam, which showed 0.49 kN/mm. For the "PFFFP-2" beam, the initial stiffness was 0.83 kN/mm, marking a 5% decrease compared to the "PPPPP-2" beam at 0.87 kN/mm.

## **Energy Dissipation Capacity**

"Oak-C" demonstrated the highest energy dissipation capacity at 1260 kN/mm, which was 30% greater than "Fir-C" at 973 kN/mm. The "OPPPO" beam dissipated 293

kN/mm of energy, which is 64% higher than the "OFFFO" beam at 179 kN/mm. "PFFFP-2" exhibited an energy dissipation capacity of 147 kN/mm, showing a 3% decrease from the "PPPP-2" beam at 152 kN/mm.

# **Comparisons Based on Inner and Outer Layers**

The beams with oak as the outer layer generally showed superior performance in ultimate load capacity and energy dissipation compared to those with fir or pine as outer layers. For example, the "OPPPO" beam (outer oak, inner pine) outperformed the "OFFFO" beam (outer fir, inner fir) by 54% in ultimate load capacity and 64% in energy dissipation. Beams with fir as the inner layers, such as the "PFFFP" and "PFFFP-2" beams, showed a slight reduction in performance compared to beams with pine as both the inner and outer layers, such as "PPPPP-2," especially in terms of initial stiffness and energy dissipation.

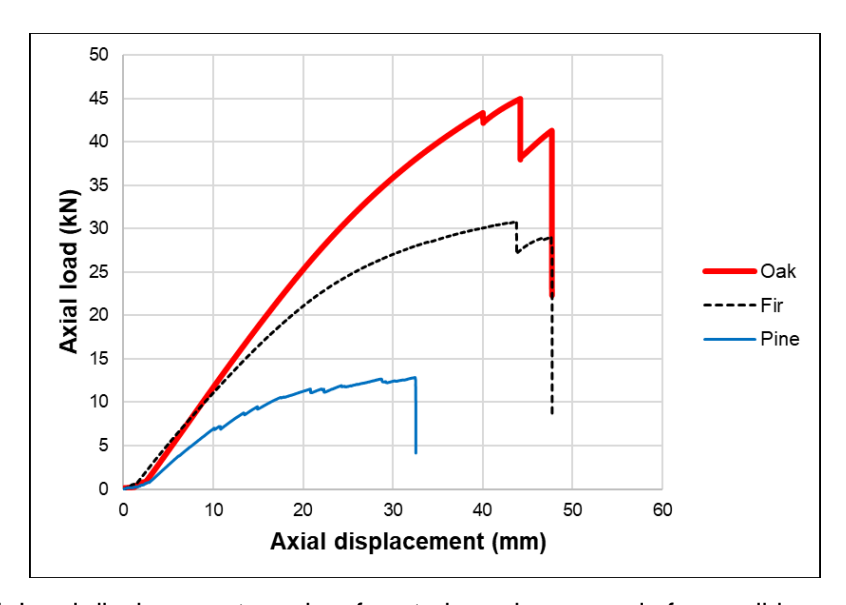


Fig. 5. Load-displacement graphs of control specimens made from solid wood

## **Overall Performance Insights**

When evaluating the overall performance of all tested specimens, it becomes evident that timber species, adhesive type, and perforation level interact in complex ways to influence the mechanical behavior of CLT beams. The "Oak-C" specimen without adhesive emerged as the strongest performer in terms of Max Load and Energy Dissipation Capacity, while perforated specimens, particularly those with PUR adhesive, tended to show reduced mechanical properties. These findings underscore the importance of careful material selection and design considerations in optimizing the structural performances of CLT beams.

The detailed experimental results for each specimen, including comparisons of max load, displacement at max load, stiffness, max displacement, and energy dissipation capacity, are presented in Table 6. The load-displacement graphs of control specimens provided in Fig. 5, specimens with PUR adhesive in Fig. 6 and specimens with PVAc adhesive in Fig. 7 illustrate differences and offering a visual representation of the mechanical responses observed during the test. Another focus of this study is to determine whether the use of different wood species in the layers leads to mechanical behavior that differs from that of the solid wood control specimens.

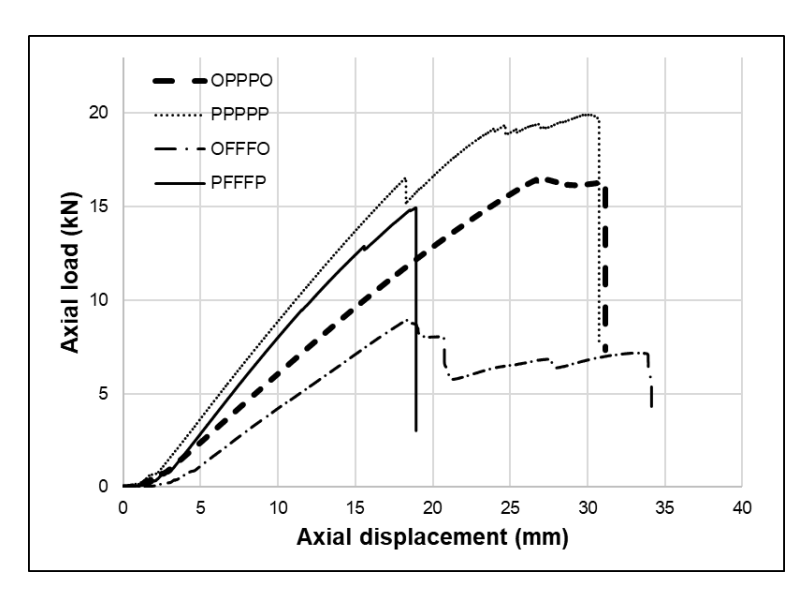


Fig. 6. Load-displacement graphs of specimens with PUR adhesive

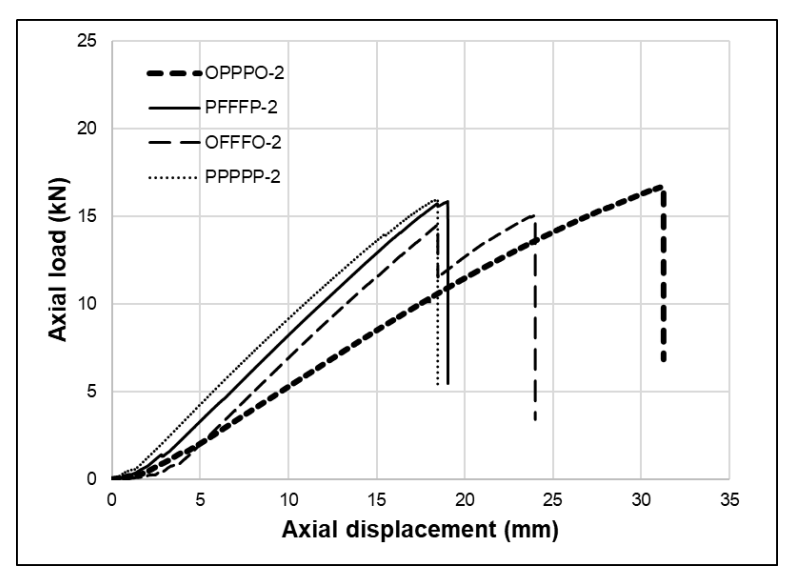


Fig. 7. Load-displacement graphs of specimens with PVAc adhesive

According to TS EN 323 (2014), statistical data on the air-dry density values of CLT beams are provided in Table 7. The table shows that the average air-dry density values of the five-layer CLT beams were lower compared to the control group of solid specimens. Among the control group, the highest average air-dry density value was found in oak wood at 0.746 g/cm³, while the lowest was in fir wood at 0.580 g/cm³. The average air-dry density values of the CLT beams also varied in parallel with the control group of solid woods.

The density value of wood material varies due to many factors, including the tree's growth location and rate, annual ring width, type of heartwood and sapwood, various extractive substances, amount of cell wall material, the age of the tree, and the locations where the tree was sourced (Kurtoğlu 1984; Bozkurt and Erdin 1989).

Literature indicates that the density of Scots pine wood ranges from 0.413 g/cm³ to 0.50 g/cm³, fir wood density ranges from 0.44 g/cm³ to 0.455 g/cm³, and oak wood density ranges from 0.62 g/cm³ to 0.71 g/cm³ (Keskin 2003; Söğütlü and Döngel 2007; Özen *et al.* 

2017). The densities of CLT beams are reported to range from 0.45 g/cm³ to 0.72 g/cm³ (Çavuş *et al.* 2024). Therefore, it has been determined that the air-dry density values of the test specimens used in this study were close to those reported in previous studies.

**Table 6.** Experimental Results

Specimen #	Name	Glue Type	Max Load (kN)	Displacement at Max Load (mm)	Stiffness (kN/mm)	Max. Displacement (mm)	Energy (kN/mm)
1	Fir-C		30.81	43.73	0.70	47.72	973.33
2	Oak-C	-	44.95	44.17	1.02	47.70	1264.07
3	Pine-C		12.86	32.44	0.40	32.54	272.78
4	OPPPO		16.51	26.90	0.61	31.15	292.51
5	PPPPP	DUD	19.94	29.79	0.67	30.74	375.09
6	OFFFO	PUR	8.95	18.36	0.49	34.13	178.52
7	PFFFP		14.95	18.88	0.79	18.92	137.02
8	OPPPO-2		16.67	31.08	0.54	31.26	267.93
9	PPPPP-2	DV/A o	15.96	18.43	0.87	18.46	151.54
10	OFFFO-2	PVAc	15.07	23.97	0.63	23.99	191.13
11	PFFFP-2		15.86	19.03	0.83	19.04	146.83

**Table 7.** Statistical Data on Air-dry Density (g/cm<sup>3</sup>) Values of CLT Beams

Specimen Group	Beam Name	N	$X_{\min}$	X <sub>max</sub>	$\overline{X}$	Std. Dev.
Control	Scots pine	5	0.573	0.608	0.588	0.017
Group	Oak	5	0.694	0.784	0.746	0.046
(Solid)	Fir	5	0.403	0.492	0.435	0.035
	PPPPP	5	0.565	0.593	0.574	0.012
5 Layer CLT	PFFFP	5	0.486	0.568	0.509	0.004
Beam	OPPPO	5	0.556	0.643	0.600	0.036
	OFFFO	5	0.511	0.567	0.539	0.030

## **NUMERICAL ANALYSIS**

In this study, numerical analyses were performed to validate the experimentally obtained data and to conduct a more detailed investigation. For the analyses, the widely used ABAQUS finite element software was chosen. First, three-dimensional models of the 11 different specimens used in the experiment were created in the ABAQUS environment. Among these, 3 were control specimens. Variations of these specimens with different properties (adhesive and wood layer types) were also added to the model, resulting in analyses for a total of 11 different scenarios. Due to the complex nature of wood material, creating an accurate material model is crucial. For this purpose, different elastic constants were defined along three main axes considering the anisotropic nature of wood. The properties of wood largely depend on the tree's trunk structure. Wood has three basic axes: Grain direction (L), radial direction (R), and tangent direction (T). While the Grain

direction (L) can be easily identified in a wood structural element, it is practically challenging to precisely determine the radial (R) and tangent (T) directions. To accurately describe the mechanical behavior of wood, nine independent elastic constants (three modulus of elasticities, three shear moduli, and three Poisson's ratios) were used. In the finite element model of wooden beams, a three-dimensional, 8-node linear brick, hexahedron element type (C3D8R) was used for wood. The load head and supports were defined as analytically rigid, and a set was created by defining a reference point to obtain the load-displacement graphics. In addition, these points were marked while constraining with analytical rigid. The points in contact with the beam were defined as hard contact and surface contact with 0.3 penalty. When defining the stress-strain relationship of wood, the tensile region was assumed to be linear-elastic, and the compressive region was assumed to be linear elastic-perfectly plastic according to the constitutive law (Fig. 8), with Eqs. 1 to 3 provided:

$$\sigma_{w,t} = E_{w,t} * \epsilon_{w,t} \tag{1}$$

$$\sigma_{wc} = E_{wc} * \epsilon_{wc} \quad if \quad \varepsilon_{wc} \le \varepsilon_{wcv} \tag{2}$$

$$\sigma_{w,c} = \sigma_{w,cy} \quad if \quad \varepsilon_{w,c} > \varepsilon_{w,cy}$$
 (3)

where  $\sigma_{w,t}$  and  $\sigma_{w,c}$  are the timber tensile and compressive stresses (MPa);  $E_{w,c}$  is the timber elasticity for compression region (MPa),  $E_{w,t}$  is the timber elasticity for tension region (MPa);  $\varepsilon_{w,t}$  and  $\varepsilon_{w,c}$  are the tensile and compressive strains (mm/mm) in timber; and  $\varepsilon_{w,c}$  is the strain (mm/mm) value at yield stress (MPa)  $\sigma_{w,c}$ .

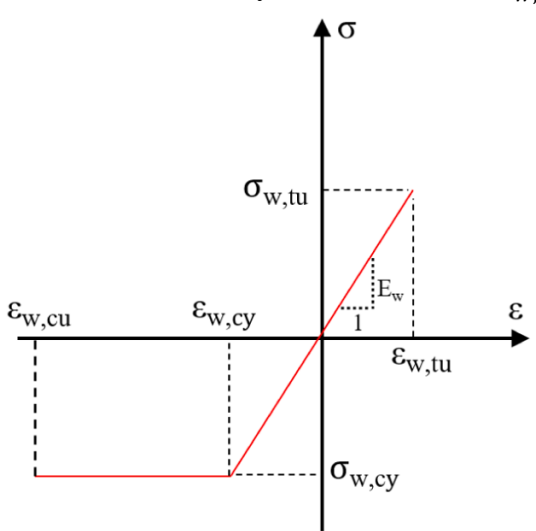


Fig. 8. Constitutive law for wood

Hill's criterion was used as the plasticity transition condition for orthotropic materials. This criterion was applied using the "Potential" sub-option in the program. The contact surfaces for laminations were defined using the cohesive zone model (CZM). Traction-separation behavior with CZM was defined in ABAQUS finite element software. This approach assumes an initial linear elastic behavior followed by the initiation and progression of damage. In the numerical analysis of CLT wooden beams using ABAQUS, it was found that beams with PVAc adhesive were more susceptible to lamination interlayer cohesive damage compared to beams with PUR adhesive. For wood laminations, a friction coefficient of 0.3 and hard contact were defined, and the cohesive parameters and damage

values used are given in Table 8. The mechanical properties of the wood models used are provided in the previously given Tables 1 to 3.

#	PUR Adh	esive	PVAc A	dhesive
	Kn (N/mm²/mm)	$\sigma_n^c$ (N/mm <sup>2</sup> )	Kn (N/mm <sup>2</sup> /mm)	$\sigma_n^c$ (N/mm²)
Mode I	3	2	15	4
	Kt (N/mm²/mm)	$\sigma_t^c$ (N/mm <sup>2</sup> )	Kt (N/mm <sup>2</sup> /mm)	$\sigma_t^c$ (N/mm <sup>2</sup> )
Mode II	20	10	100	25

Table 8. Cohesive Parameters Used for Mode I and Mode II

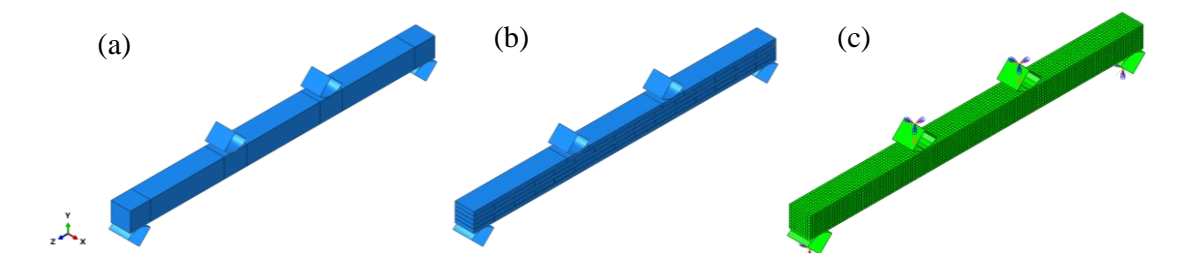


Fig. 9. Finite element model with (a) control (b) 5-layer (c) mesh

Finite element models were meshed into smaller parts to obtain more accurate results while considering the analysis time. In this study, the finite element size for wood specimens was set to 15 mm. A photo showing the mesh structure of control and 5-layer CLT wooden beams is provided in Fig. 9. Some studies (Nowak *et al.* 2013; Guo *et al.* 2019) have ended their analyses after reaching the ultimate load to compare with experimental specimen results. Similarly, this study was concluded after reaching the ultimate load. Comparative load-displacement graphs of experimental results and numerical analyses for reference (control) specimens are shown in Fig. 10. Comparative load-displacement graphs for 5-layer CLT beams are provided in Fig. 11 for PUR adhesive and Fig. 12 for PVAc adhesive. Von-Mises stress distributions for CLT beams are shown in Fig. 13 for control specimens and Fig. 14 for 5-layer CLT beams. A comparative visual of the experimental and numerical models for the PFFFP specimen is shown in Fig. 15.

Comparative results of numerical analyses and experiments are provided in Table 9. According to the ratio values in the table, experimental and numerical results generally showed consistency. For maximum load, there were less than 20% differences between experimental and numerical results for most specimens, indicating that the model is generally reliable. However, for displacement values, larger differences, such as a 25% deviation for the "OFFFO" specimen, were observed. This is thought to be due to mechanical properties along the fiber direction specific to the OFFFO CLT beam or some structural defects, resulting in different outcomes compared to the finite element analysis. In stiffness values, numerical analyses generally provided results up to 20% higher than experimental results, indicating that modeling may overestimate stiffness in some situations. Maximum displacement ratios are generally quite close with differences of less than 10%. Energy dissipation capacity is where the largest differences were observed, with deviations reaching up to 30% in "OFFFO" and "PFFFF" specimens. These results suggest that, considering possible experimental imperfections, the numerical model is generally reliable.

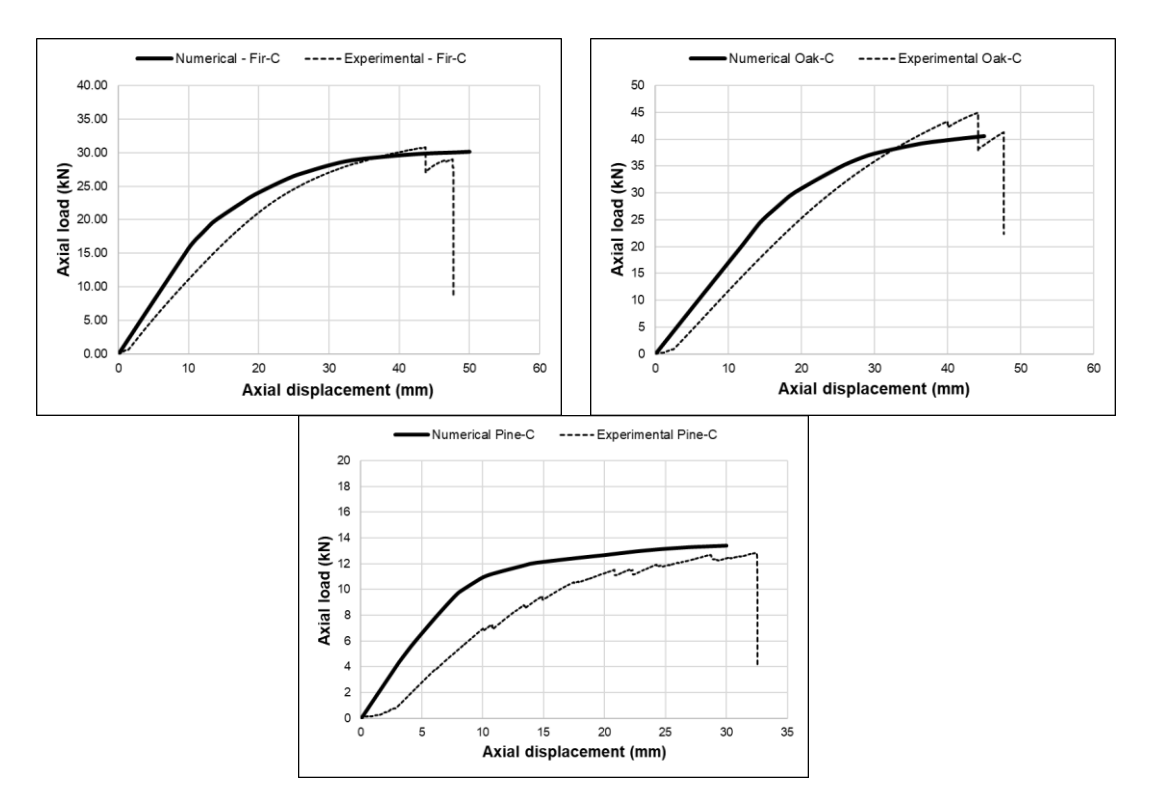
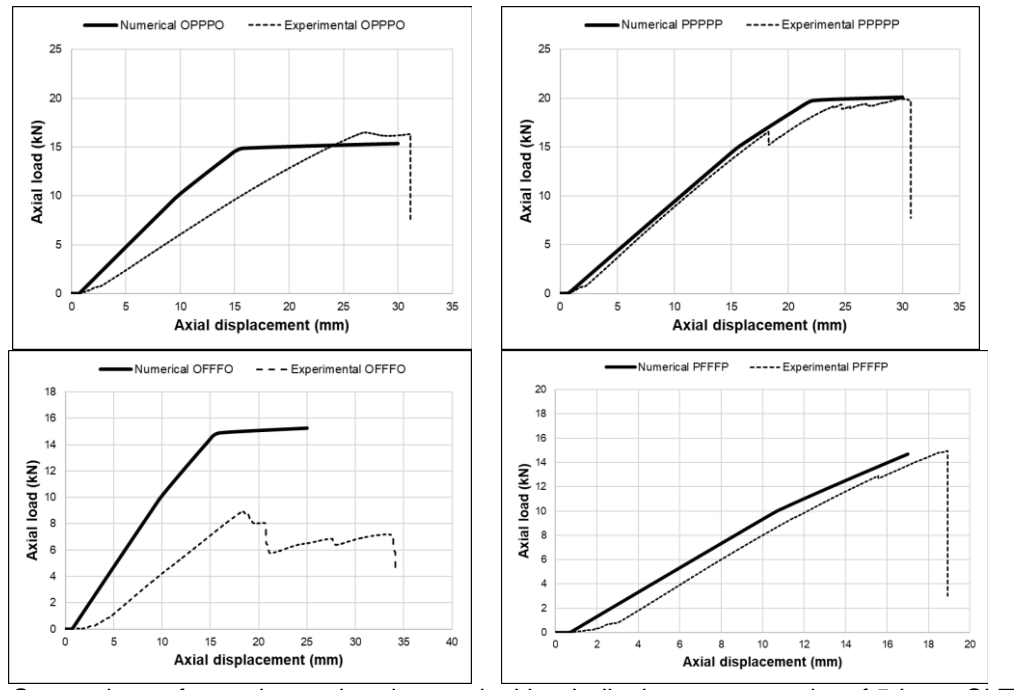
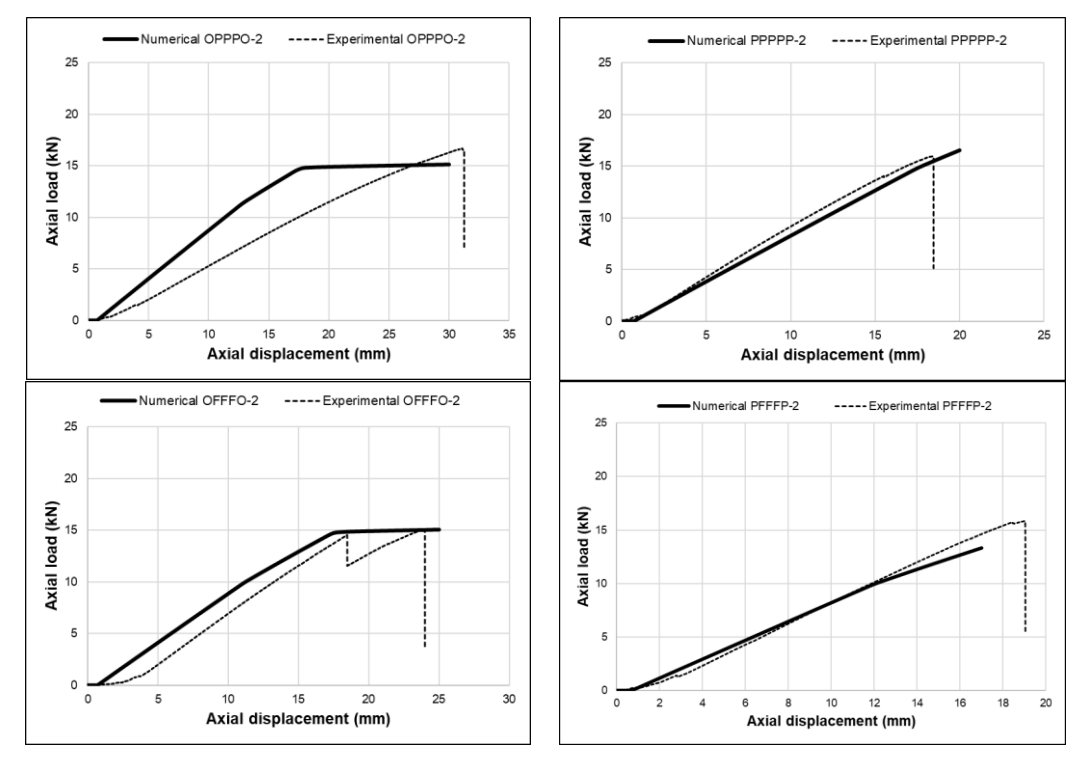


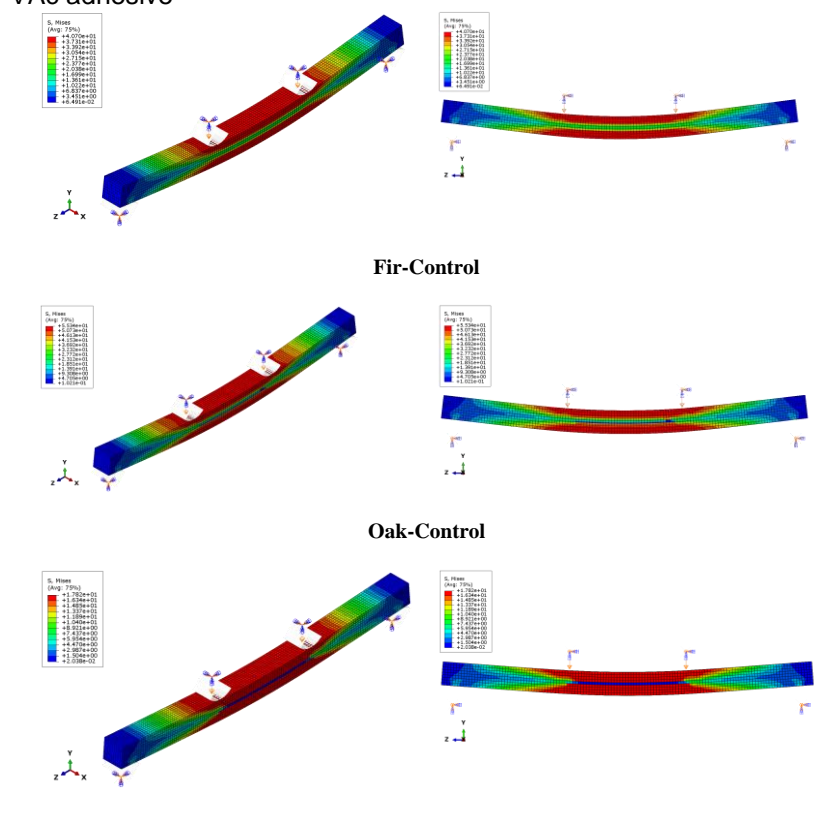
Fig. 10. Comparison of experimental and numerical load–displacement graphs of solid wood control beams



**Fig. 11.** Comparison of experimental and numerical load–displacement graphs of 5-layer CLT beams with PUR adhesive



**Fig. 12.** Comparison of experimental and numerical load–displacement graphs of 5-layer CLT beams with PVAc adhesive



Pine-Control Fig. 13. Von-Mises stress distributions of CLT control beams

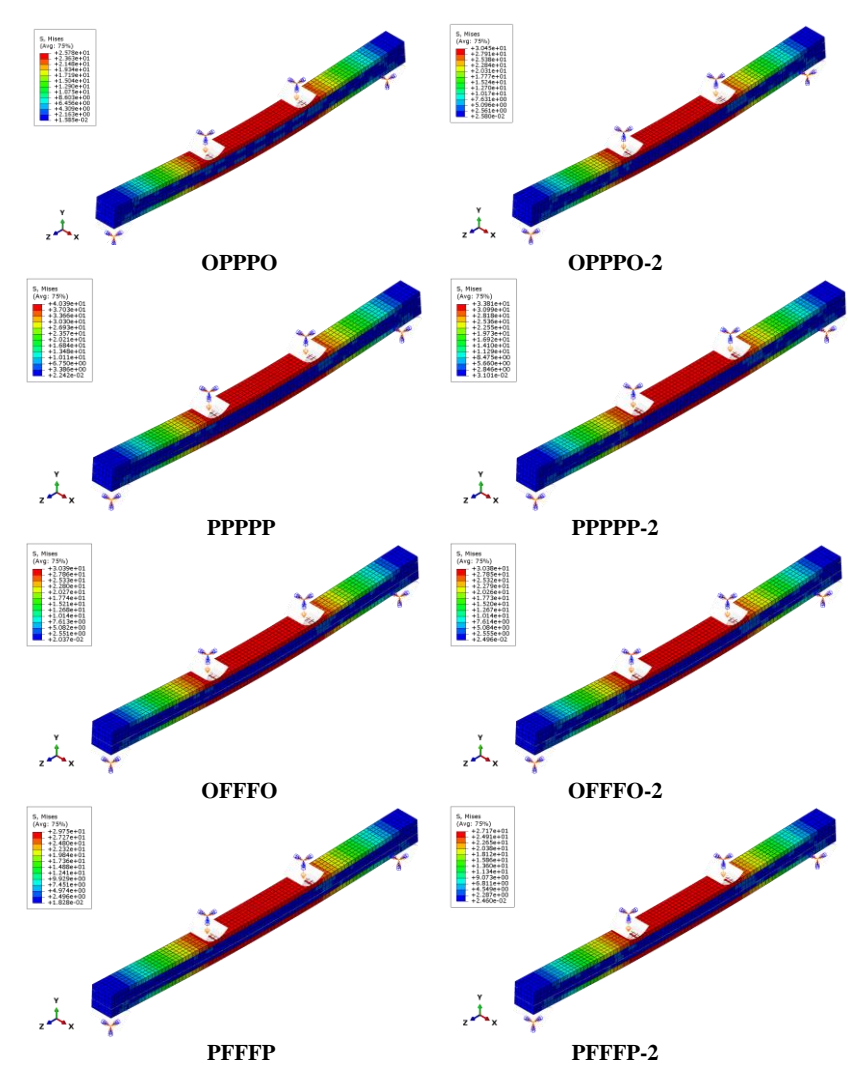


Fig. 14. Von-Mises stress distributions of CLT 5-Layer beams

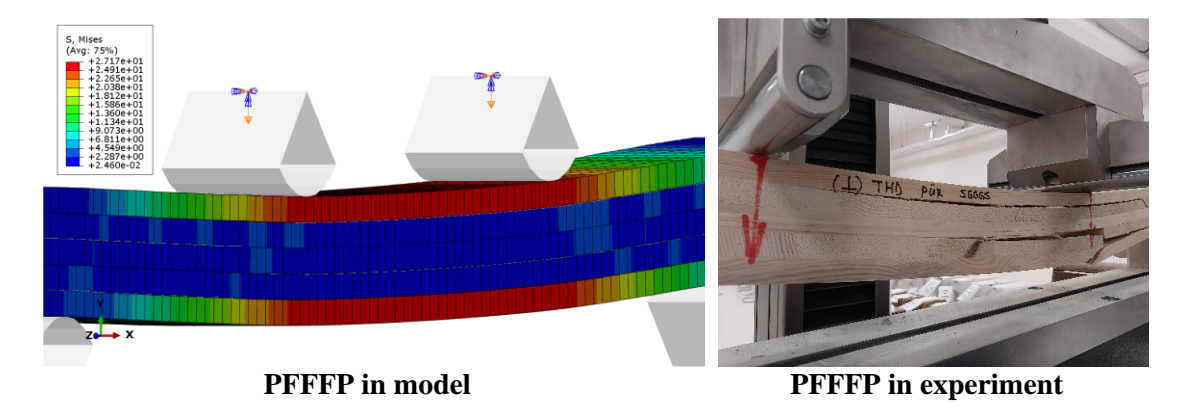


Fig. 15. Von-Mises stress distributions vs. experiment

Table 9. Comparative Results of Numerical Analysis and Experiments

Spec.	Glue Type	Ма	ax Load (kN)			Displacement at Max Load (kN/mm)			Disp	Max. placement (mm)		Energy Dissipation Capacity (kN/mm)				
		Exper.	Num.	Rat.	Exper.	Num.	Rat.	Exper.	Num.	Rat.	Exper.	Num.	Rat.	Exper.	Num.	Rat.
Fir-C		30.81	30.14	1.02	43.73	50.00	0.87	0.70	0.60	1.17	47.72	50.00	0.95	973.33	1136.30	0.86
Oak-C	-	44.95	40.56	1.11	44.17	45.00	0.98	1.02	0.90	1.13	47.7	45.00	1.06	1264.07	1265.40	1.00
Pine-C		12.86	13.41	0.96	32.44	30.00	1.08	0.40	0.45	0.89	32.54	30.00	1.08	272.78	313.78	0.87
OPPPO		16.51	15.37	1.07	26.9	30.00	0.90	0.61	0.51	1.20	31.15	30.00	1.04	292.51	336.97	0.87
PPPPP	PUR	19.94	20.10	0.99	29.79	30.00	0.99	0.67	0.67	1.00	30.74	30.00	1.02	375.09	383.44	0.98
OFFFO	PUR	8.95	15.25	0.59	18.36	25.00	0.73	0.49	0.61	0.80	34.13	25.00	1.37	178.52	259.45	0.69
PFFFP		14.95	14.69	1.02	18.88	17.00	1.11	0.79	0.86	0.92	18.92	17.00	1.11	137.02	128.26	1.07
OPPPO		16.67	15.12	1.10	31.08	30.00	1.04	0.54	0.50	1.06	31.26	30.00	1.04	267.93	317.29	0.84
PPPPP	DV/A =	15.96	16.53	0.97	18.43	20.00	0.92	0.87	0.83	1.05	18.46	20.00	0.92	151.54	164.36	0.92
OFFFO	PVAc	15.07	15.04	1.00	23.97	25.00	0.96	0.63	0.60	1.04	23.99	25.00	0.96	191.13	242.67	0.79
PFFFP		15.86	13.32	1.19	19.03	17.00	1.12	0.83	0.78	1.06	19.04	17.00	1.12	146.83	114.62	1.28

## DISCUSSION OF RESULTS BASED ON GLUE LINE DIRECTION

In CLT beams, although the application load is generally applied perpendicular to the adhesive line, this section experimentally examines the loading situation applied parallel to the adhesive line. Multiple variance analysis was performed to determine whether the effects of these loading conditions on the load-bearing capacity of the beams were significant. Based on the results of the multiple variance analysis, Duncan's test was conducted to identify differences among groups where effects were found to be significant. Descriptive statistics of the data obtained from the conducted experiments were performed, and multiple variance analyses were conducted to evaluate the differences between the data. Statistical analyses were performed using the MSTAT-C and SPSS programs.

Table 10. Comparative Experimental Results Based on Glue Directions

Specimen	Name	Glue Type	Direction	Max Load (kN)	Displacement at Max Load (mm)	Stiffness (kN/mm)	Max. Displacement (mm)	Energy (kN/mm)
1	Fir-C			30.81	43.73	0.705	47.72	771.23
2	Oak-C	-	-	44.95	44.17	1.018	47.7	731.74
3	Pine-C			12.86	32.44	0.396	32.54	205.26
4	OPPPO			16.51	26.9	0.614	31.15	292.51
5	PPPPP	PUR		19.94	29.79	0.669	30.74	375.09
6	OFFFO	PUR		8.95	18.36	0.487	34.13	178.52
7	PFFFP		Perpendicular	14.95	18.88	0.792	18.92	137.02
8	OPPPO-2		to the Glue Line	16.67	31.08	0.536	31.26	267.93
9	PPPPP-2	D\/Δc		PVAc	15.96	18.43	0.866	18.46
10	OFFFO-2	FVAC		15.07	23.97	0.629	23.99	191.13
11	PFFFP-2			15.86	19.03	0.833	19.04	146.83
12	OPPPO			19.32	27.16	0.711	28.06	168.21
13	PPPPP	PUR		21.73	26.11	0.832	30.3	224.65
14	OFFFO	PUR		19.6	30.11	0.651	35.71	225.08
15	PFFFP		Parallel to the	18.77	29.46	0.637	31.03	194.96
16	OPPPO		Glue Line	14.43	22.22	0.649	22.45	142.98
17	PPPPP	D) / A =		19.1	29.94	0.638	38.62	306.01
18	OFFFO	PVAc		10.75	27.76	0.387	27.77	118.67
19	PFFFP			17.69	29.24	0.605	46.62	366.47

According to Table 10, it was found that the ultimate load capacity, displacement at ultimate load, initial stiffness, and energy dissipation capacity obtained from the four-point bending tests of five-layer cross-laminated wooden beams were different from each other. The effects of parameters making up the beams and the direction of applied forces on the load-bearing capacity of the beams were determined using multiple variance analysis, and the results are provided in Table 11. According to the multiple variance analysis results, the effects of the wood type in the outer layer, the wood type in the inner layer, and the force directions applied to the adhesive lines in CLT beams were statistically significant (p<0.05). The variance analysis results indicated that the effect levels (F:18.105;

F:19.063) of the force directions applied to determine load-bearing capacity in the outer layer of the beams were higher than those of all other parameters. Based on the multiple variance analysis results, Duncan's test was performed to determine the differences among the groups where effects were found to be significant, and homogeneous groups were identified as presented in Table 12. According to Duncan's test results, depending on the direction of the applied force, it was found that the load-bearing capacity of CLT beams exposed to bending load parallel to the adhesive line (39.81 N/mm²) was higher than that perpendicular to the adhesive line.

Variances	Sum of Squares	SD	Mean of Squares	F	Level of Significance (p<0,05)
Glue (A)	19.751	1	19.751	0.612	0.445
Force Direction (B)	584.359	1	584.359	18.105	0.001*
Outer Layer (C)	615.275	1	615.275	19.063	0.000*
Inner Layer (D)	272.607	1	272.607	8.446	0.010*
A * B	97.819	1	97.819	3.031	0.101
A * C	11.325	1	11.325	0.351	0.562
A * D	78.289	1	78.289	2.426	0.139
B * C	0.003	1	0.003	0.000	0.992
B * D	46.244	1	46.244	1.433	0.249
C * D	2.297	1	2.297	0.071	0.793
A * B * C	15.391	1	15.391	0.477	0.500
A* B * D	134.912	1	134.912	4.180	0.058
A * C * D	43.008	1	43.008	1.333	0.265
B * C * D	2.619	1	2.619	0.081	0.779
A * B * C* D	2.715	1	2.715	0.084	0.776
Error	516.423	16	32.276		
Total	42851.238	32			

 Table 11. Multivariate Analysis of Bending Strength Values of CLT Beams

Previous studies have determined that the load-bearing capacity parallel to the fibers in laminated wood beams is higher than that perpendicular to the fibers (Oran 2012; Uzel 2015). When used in structural applications, one must be aware of which direction the applied load affects, as it is subjected to static load-bearing capacity (Borůvka *et al.* 2020). Furthermore, studies have noted that static load-bearing capacity is generally higher in the radial direction for many wood materials.

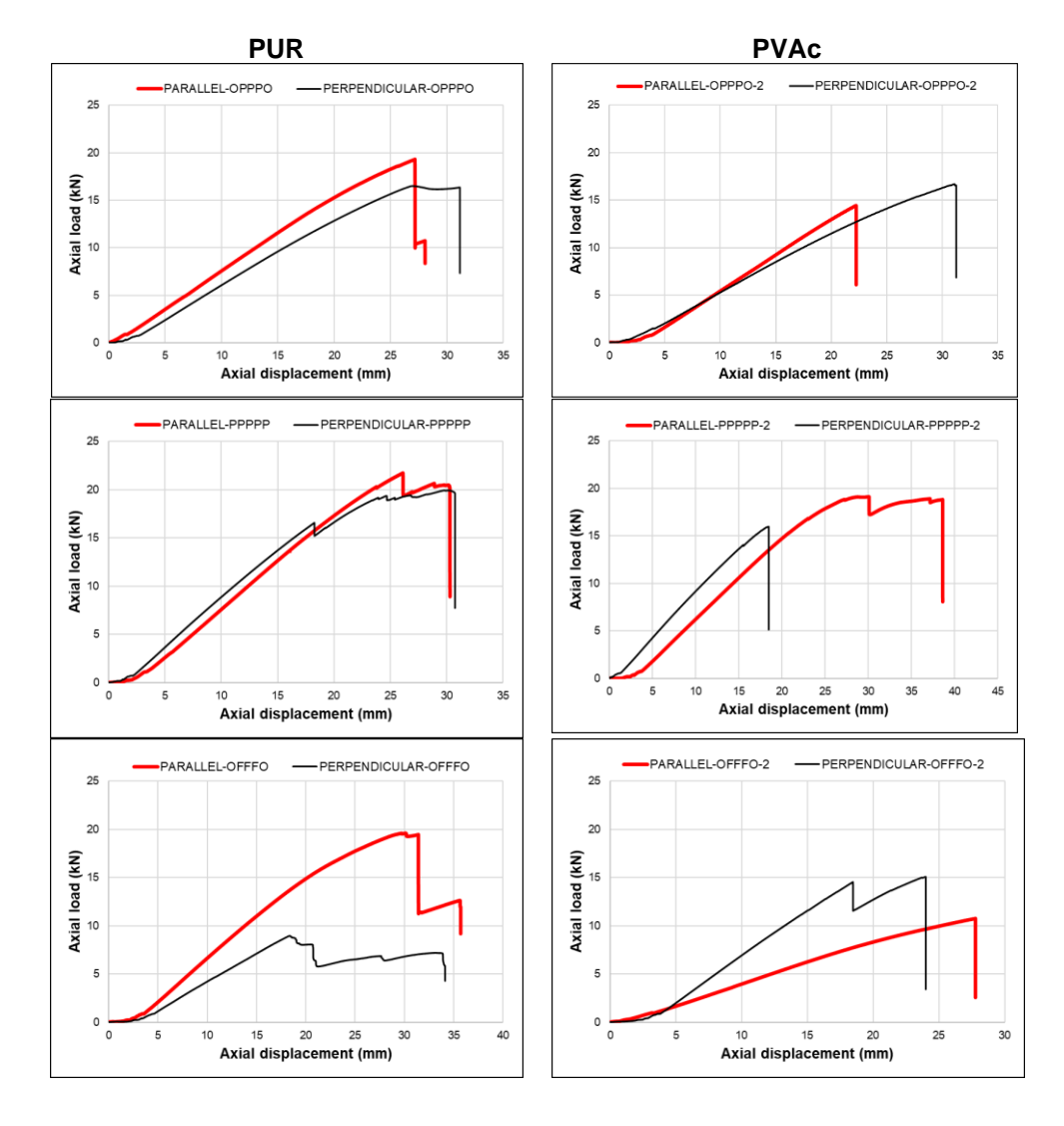
In this study, the high load-bearing capacity parallel to the adhesive line can be attributed to the fact that the force applied due to the perpendicular positioning of the layers in CLT beams acts perpendicularly to the layers' surfaces.

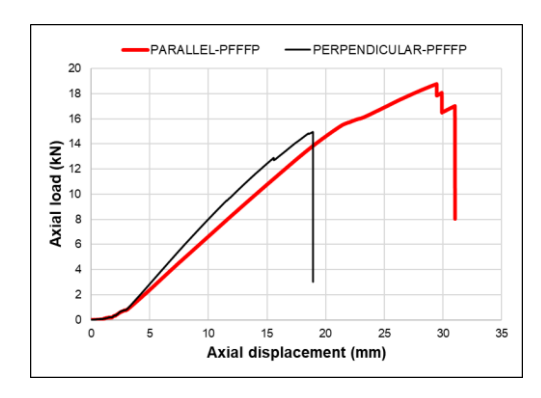
In wood materials with the same moisture content, the main factors affecting resistance values are density, the proportion of latewood, temperature level and wood type, age of the wood, heartwood and sapwood ratio, anatomical and chemical structure, or structural application form (Bektaş 1997; Yalınkılıç 1998).

It can be said that load-bearing capacity resulting from the external and internal wood types in the laminations increase inversely with density. According to the studies, wood with more cell voids absorbs more adhesive, resulting in greater penetration of adhesive into the cell voids and an increase in cohesive strength. Thus, wood types with higher specific gravity and cell voids also show increased load-bearing capacity in laminations (Kasal *et al.* 2010; Kesik *et al.* 2016).

**Table 12.** Homogeneity Groups based on Duncan Test of Variances whose Effects were found to be Significant according to Multiple Variance Analysis Test

Direction of Force Application	N	$\overline{X}$ (N/mm <sup>2</sup> )	HG				
Parallel to Glue Line	16	39.81	Α				
Perpendicular to Glue Line	16	31.26	В				
	LSD: 4.096 N/m	nm²					
Outer Layer Wood Type							
Scots Pine	16	39.92	Α				
Oak	16	31.15	В				
	LSD: 4.096 N/m	ım2					
Inner Layer Wood Type							
Scots Pine	16	38.45	А				
Fir	16	32.62	В				
LSD: 4.096 N/mm <sup>2</sup>							





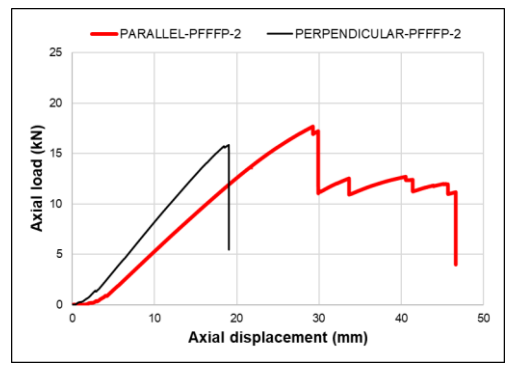


Fig. 16. Load-displacement graphs according to glue directions

Reviewing the experimental data in Table 10, it is evident that whether the loading direction was parallel or perpendicular to the adhesive line led to distinct differences in specimen performance. In terms of maximum load capacity, specimens subjected to perpendicular loading generally showed lower capacity values. For example, the OFFFO specimen had a maximum load capacity of 8.95 kN under perpendicular loading, while this value increased to 19.6 kN under parallel loading. A similar situation was observed in the PFFFF specimen, where the capacity under perpendicular loading was 14.4 kN and increased to 17.7 kN under parallel loading. Looking at displacement values, specimens subjected to parallel loading generally showed higher displacements. For example, the "OFFFO" specimen's displacement was 18.9 mm under perpendicular loading and increased to 31.1 mm under parallel loading. Similarly, the "PFFFF" specimen's displacement increased from 22.2 mm under perpendicular loading to 29.2 mm under parallel loading. In conclusion, parallel and perpendicular loadings created significant differences in the mechanical performance of the specimens. Parallel loadings generally resulted in higher maximum loads, greater displacements, and higher energy dissipation capacity, while perpendicular loadings showed lower stiffness and energy capacity. This indicates that the loading direction is a critical parameter to consider in the design of wood composite materials. Load-displacement graphs according to adhesive directions are comparatively shown in Fig. 16.

#### **CONCLUSIONS**

This study provided a comprehensive evaluation of how different adhesive types and wood layer configurations affect the mechanical performance of cross-laminated timber (CLT) beams. The main findings are summarized below.

 Beams with polyurethane (PUR) adhesive and oak outer layers demonstrated higher ultimate load and energy dissipation capacities compared to beams with pine layers. However, it was found that perforation negatively affected performance in both adhesive types. The use of fir inner layers led to small increases in displacement capacity but resulted in slight decreases in stiffness and energy dissipation capacity. Numerical analysis results, consistent with experimental data, highlight the importance of selecting appropriate adhesives and wood types to optimize the

- mechanical performance of CLT beams. These findings provide valuable insights for optimizing CLT beam design in practical applications.
- 2. In the study, reductions in load-bearing capacity were observed in cross-laminated wooden beams made from yellow pine, spruce, and oak compared to solid control specimens. The load-bearing capacity of CLT beams with yellow pine and oak in the outer layers was found to be higher for yellow pine wood. The load-bearing capacity of CLT beams with yellow pine in the inner layer was found to be higher than that of spruce wood.
- 3. In the experimental study based on adhesive line direction, the load-bearing capacity of cross-laminated beams parallel to the adhesive line was higher compared to the perpendicular direction.
- 4. Numerical analysis of CLT wooden beams using ABAQUS finite element software showed that accurate and realistic results could be achieved. The finite element model created with ABAQUS showed that the ultimate load capacity, displacement, and energy consumption capacities of CLT wooden beams were highly consistent with experimental results.
- 5. The cohesive zone model (CZM) used in ABAQUS finite element software successfully managed the interactions between CLT beams.
- 6. The average ratio values of the experimental results and analyses using ABAQUS were 1.00 for ultimate load capacity, 0.97 for displacement at ultimate load, 1.03 for initial stiffness, and 0.92 for energy dissipation capacity.

#### **ACKNOWLEDGMENTS**

The study was supported by the Gazi University Scientific Research Project unit within the scope of the ID: 8051 / FDK-2022-8051 project, and the authors would like to thank Gazi University for their support.

## REFERENCES CITED

- Abed, J., Rayburg, S., Rodwell, J., and Neave, M. (2022). "A review of the performance and benefits of mass timber as an alternative to concrete and steel for improving the sustainability of structures," *Sustainability* 14, article 5570. DOI: 10.3390/su14095570
- ANSI/APA PRG 320 (2018). Standard for Performance-Rated Cross-Laminated Timber, APA-The Engineered Wood Association, Tacoma, WA.
- Bektaş, İ. (1997). *Technological Properties of Red Pine Wood and Their Changes According to Regions*, PhD Thesis, Istanbul University, Institute of Science, Istanbul, Turkey.
- Borůvka, V., Novák, D., and Šedivka, P. (2020). "Comparison and analysis of radial and tangential bending of softwood and hardwood at static and dynamic loading," *Forests* 11(8), 896. DOI: 10.3390/f11080896.
- Bozkurt, Y., and Erdin, N. (1989). "Wood material quality and silvicultural measures," *Journal of the Faculty of Forestry Istanbul University* 39(3), 1-13.

- Brandner, R., Flatscher, G., Ringhofer, A., Schickhofer, G., and Thiel, A. (2016). "Cross laminated timber (CLT): Overview and development," *European Journal of Wood and Wood Products* 74, 331-351. DOI: 10.1007/s00107-015-0999-5
- BS EN 301 (2010). Adhesives, Phenolic and Aminoplastic, for Load-bearing Timber Structures Classification and Performance Requirements, British Standards Institution, London, UK.
- Callegari, G., Cremonini, C., Rocco, V. M., Spinelli, A., and Zanuttini, R. (2010). "The production of hardwood X-Lam panels to valorise the forest-wood chain in Piemonte (Italy)," *Proceedings of the 11th WCTE*, Italy, 1617-1622.
- Çavuş, Z., Kaya, M., and Bülbül, R. (2024). "Investigation of the effects of perforation applied to the intermediate layers of cross-laminated timber (CLT) panels on sound absorption coefficient," *Anadolu Journal of Forest Research* 9(2), 75-81. DOI: 10.53516/ajfr.1385796.
- Ceylan, A. (2021). Experimental Investigation of Cross-Laminated Timber Panel Systems and Connection Properties, Doctoral dissertation, Turkey.
- Crespell, P., and Gagnon, S. (2010). *Cross Laminated Timber: A Primer*, Special Publication 52, FPInnovations, Canada, pp. 1-2.
- Dönmez, T. Ü., Türer, A., Anil, Ö., and Erdem, R. T. (2022). "Experimental and numerical investigation of timber formwork beam under different loading type," *Mechanics Based Design of Structures and Machines* 50(3), 1090-1110. DOI: 10.1080/15397734.2020.1749071
- FPInnovations (2011). *CLT Handbook: Cross-Laminated Timber*, S. Gagnon and C. Pirvu (Eds.), Special Publication SP-528 E, Quebec, Canada.
- Gavric, I. (2013). *Seismic Behavior of Cross-Laminated Timber Buildings*, PhD Thesis, University of Trieste, Italy.
- Guo, N., Wang, W., and Zuo, H. (2019). "Flexural property of string beam of prestressed glulam based on influence of regulation and control," *Structural Durability and Health Monitoring* 13(2), 143. DOI: 10.32604/sdhm.2019.04640
- He, M., Sun, X., and Li, Z. (2018). "Bending and compressive properties of cross-laminated timber (CLT) panels made from Canadian hemlock," *Construction and Building Materials* 185, 175-183. DOI: 10.1016/j.conbuildmat.2018.07.072.
- Kasal, A., Hasan, E. F. E., and Dizel, T. (2010). "Determination of bending strength and modulus of elasticity in solid and laminated wood materials," *Politeknik Dergisi* 13(3), 183-190.
- Kesik, H. İ., Keskin, H., Temel, F., and Öztürk, Y. (2016). "Surface roughness and adhesion strength of some wood species impregnated with Vacsol Aqua," *Kastamonu University Journal of Forestry Faculty* 16(1), 30-39. DOI: 10.17475/kujff.75845.
- Keskin, H. (2003). "Some physical and mechanical properties of laminated oriental spruce wood," *Süleyman Demirel University Journal of Forestry Faculty Series A* 1, 139-151.
- Kurtoğlu, A. (1984). "Wood-weight relationships," *Journal of the Faculty of Forestry Istanbul University* 34(1), 150-163.
- Lehmann, S. (2013). "Low carbon construction systems using prefabricated engineered solid wood panels for urban infill to significantly reduce greenhouse gas emissions," *Sustainable Cities and Society* 6, 57-67. DOI: 10.1016/j.scs.2012.08.004
- Mercimek, Ö., Ghoroubi, R., Akkaya, S. T., Türer, A., Anıl, Ö., and İşleyen, Ü. K. (2024). "Flexural behavior of finger joint connected glulam wooden beams

- strengthened with CFRP strips," *Structures* 66, 106853. DOI: 10.1016/j.istruc.2024.106853
- Milner, H. R. (2009). "Sustainability of engineered wood products in construction," in: *Sustainability of Construction Materials*, J. A. Khatib (ed.), Woodhead, Sawston, UK, pp. 184-212. DOI: 10.1533/9781845695842.184
- Nowak, T. P., Jasieńko, J., and Czepiżak, D. (2013). "Experimental tests and numerical analysis of historic bent timber elements reinforced with CFRP strips," *Construction and Building Materials* 40, 197-206. DOI: 10.1016/j.conbuildmat.2012.09.106
- Oran, B. (2012). Some Technological Properties of Cross-Laminated Timber Made from Coconut (Cocos nucifera L.) Wood, Master's thesis, Institute of Science, Turkey.
- Özen, Z. E., Onat, S. M., and Aydemir, D. (2017). "Effects of thermal treatment on some properties of Scots pine and Uludag fir woods," *Bartın Journal of Forestry Faculty* 19(1), 187-193. DOI: 10.24011/barofd.313318.
- Perez-Garcia, J., Lippke, B., Briggs, D., Wilson, J., Bowyer, J., and Meil, J. (2005). "The environmental performance of renewable building materials in residential construction," *Wood and Fiber Science* 37, 3-17.
- Ross, R. J. (2010). *Wood Handbook: Wood as an Engineering Material*. USDA Forest Service, Forest Products Laboratory, General Technical Report FPL-GTR-190, 2010: 509 p. 1 v., 190. DOI: 10.2737/FPL-GTR-190
- Sonderegger, W., Kránitz, K., Bues, C. T., and Niemz, P. (2015). "Aging effects on physical and mechanical properties of spruce, fir and oak wood," *Journal of Cultural Heritage* 16(6), 883-889. DOI: 10.1016/j.culher.2015.02.002
- Söğütlü, C., and Döngel, N. (2007). "Tensile shear strengths of some native woods bonded with PVAc and polyurethane adhesives," *Politeknik Dergisi* 10(3), 287-293.
- Türer, A., Anil, Ö., Cevik, A., and Erdem, R. T. (2024). "Investigation of damaged formwork timber beam retrofitting with anchored CFRP strip under different loading," *Steel and Composite Structures* 50(6).
- TSE (1999). TS EN 323: Wood-based Panels Determination of Density, Turkish Standards Institution, Ankara, Turkey.
- Uzel, M. (2015). Effect of Supporting Layers and Lamella Thickness on Mechanical Properties of Laminated Timber Elements, Master's thesis, Turkey.
- Waugh Thistleton Architects (2018). *100 Projects UK CLT*, Think Wood, Canada, pp. 68-70. Available at: https://www.thinkwood.com/wp-content/uploads/2019/08/Think-Wood-Publication-100-Projects-UK-CLT.pdf.
- Yalınkılıç, B. (1998). "Enhancement of the biological resistance of wood by phenylboronic acid treatment," *Journal of Wood Science* 44(2), 152-157. DOI: 10.1007/BF00526262
- Yesügey, S. C., Karaman, Ö. Y., and Güzel, N. (2014). *Wood Material Housing Technology*, Yalın Yayıncılık, Istanbul, Turkey.

Article submitted: March 7, 2025; Peer review completed: April 19, 2025; Revised version received and accepted: April 24, 2025; Published: May 1, 2025. DOI: 10.15376/biores.20.2.4720-4745